J Inorg Organomet Polym ##################
DOI: 10.1007/s10904-013-####-##

Encapsulation of Au Nanoparticles by Poly(4-vinylpyridine)-*block*-Polystyrene-*block*-Poly(4-vinylpyridine) for Controlled Chain Assembly

Cuicui Liu · Jun Xu · Hongyu Chen

Received: ##### 2014 / Accepted: ###### 2014 / Published online: ####### 2014

Abstract We report a facile method to encapsulate Au nanoparticles (NPs) in an amphiphilic ABA triblock copolymer, poly(4-vinylpyridine)-*block*-polystyrene-*block*-poly(4-vinylpyridine), (P4VP-*b*-PS-*b*-P4VP), forming Au@P4VP-*b*-PS-*b*-P4VP core-shell nanostructures. On the basis of the hydrophobically funcationalized Au surface, we propose that the P4VP-*b*-PS-*b*-P4VP is folded into a U shape, so that the hydrophobic PS block attach to the Au surface and the hydrophilic P4VP blocks are dissolved in the solution facing outwards. As the polymer micelles transform from spheres to cylinders and vesicles, the embedded Au NPs are brought along in the process and end up in the complex polymer nanostructures. Driven by the tendency of the polymer to form cylindrical micelles, the positively charged core-shell NPs can assemble into chains, where the method was only demonstrated previously exploiting the negatively charged amphiphilic polystyrene-*block*-poly(acrylic acid) shells.

Keywords Poly(4-vinylpyridine)-*block*-polystyrene-*block*-poly(4-vinylpyridine) · ABA triblock copolymer · Nanoparticle · Self-assembly · Hybrid nanostructure

[*] C. Liu, J. Xu, H. Chen (✉)
Division of Chemistry and Biological Chemistry
Nanyang Technological University
21 Nanyang Link, Singapore 637371
Fax: (+65) 67911961
E-mail: hongyuchen@ntu.edu.sg
Web: http://www.ntu.edu.sg/home/hongyuchen/

1 Introducion

Amphiphilic block copolymers (BCPs) have been extensively studied and used for preparing polymer micelles with different morphologies and functions [1-3]. In a selective solvent, their insoluble blocks are squeezed in the core and the soluble blocks are dissolved in the solvent as the corona, forming various micelle structures such as sphere, cylinder, lamella, and vesicle [4-7]. As such, the surface functional group of the micelles are determined by the chemical nature of the hydrophilic blocks.

Incorporating NPs into the BCP micelles is a convenient approach to hybrid nanostructures. Owing to their small size and size-dependent properties, the NPs have been applied in many areas such as sensing, labelling, imaging, cell separation and photodynamic therapy [8-12]. A major challenge for using NPs in these applications is to ensure their colloidal stability, which can be greatly enhanced with a conformal coating. A wide range of methods have been developed to encapsulate various kinds of NPs in polymer [13-15], lipid [16], and inorganic shells [17-19]. In comparison, polymer encapsulation is facile and versatile, and the resulting shells are robust with rich morphologies.

Attempts have been made to embed NPs in BCP micelles. One approach is to synthesize NPs *in situ* in/on the BCP micelles, where metal ions are first adsorbed in the polymer aggregates followed by chemical reductions [20-21]. For example, polystyrene-*block*-polyvinylpyridine (PS-*b*-P4VP) can give rise to sphere, cylinder and lamella [21]. Inorganic precursors such as Au, Ag and Pd ions can be adsorbed in the P4VP blocks and reduced to give metal NPs. However, this method cannot give uniform sized NPs and other types of BCP micelles cannot be readily used. Alternatively, prefabricated NPs can be encapsulated in BCP micelles, requiring the controlled assembly of the micelles in the presence of the NPs [14-15, 22-27]. Taton et al. showed that a variety of NPs, including Au, γ-Fe_2O_3, and carbon nanotube, can be encapsulated in polystyrene-*b*-poly(acrylic acid) (PSPAA) shells using a self-assembly approach; the assembled hybrids could be permanently fixed by cross-linking the soluble PAA block [13, 25-27]. In addition, co-assembly of polymer-decorated NPs with amphiphilic copolymer gave cylindrical and vesicular micelles, where the NPs were embedded in the centre of the polymer domains [28-30].

Our group studied the mechanisms of encapsulating NPs in PSPAA micelles. Hydrophobic ligands were used to tune the NP-polymer interfacial energy; mixed solvent and high temperature were used to ensure sufficient mobility of the polymer during its self-assembly and shape transformation, so that Au@PSPAA core-shell NPs were directly obtained as the thermodynamically controlled product [14-15, 31-34]. As a new approach of NP self-assembly, the purified Au@PSPAA NPs were subjected to acidic conditions, causing the formation of ultralong NP chains [35]. The mechanistic details of the structural transformation from spherical PSPAA micelles to cylinders and vesicles were also carried out [36-37].

In this work, we use a positively charged triblock copolymer, $P4VP_{43}$-*b*-PS_{260}-*b*-$P4VP_{43}$ for making Au-polymer hybrids. Considering that only the negatively charged PSPAA was used in our previous studies, the new results provide strong support for the general mechanistic principles in our system. With the different type of polymer, we demonstrate that (1) full encapsulation of the Au NPs can be achieved [14]; (2) Au NPs can be incorporated in cylindrical and vesicular micelles [36]; and (3) the Au@P4VP-PS-P4VP NPs can be assembled into chains as a result of forming polymer cylinders [35].

2 Experimental

2.1 Materials

All chemical reagents were used without further purification. Amphiphilic triblock copolymer $P4VP_{43}$-*b*-PS_{260}-*b*-$P4VP_{43}$, (M_n=27000 for the polystyrene block and M_n=4500 for the poly(4-vinylpyridine) block, M_w/M_n=1.09) was purchased from Polymer Source. 2-Dipalmitoyl-sn-glycero-3-phosphothioethanol (sodium salt) (ligand **1**) was purchased from Avanti Polar Lipids. 2-Naphthalenethiol (ligand **2**), tetrakis(hydroxymethyl)-phosphonium chloride (THPC, 80% in H_2O) and cetyltrimethylammonium bromide (CTAB) were purchased from Sigma-Aldrich. Deionized water (resistance > 18.2 MΩ•cm^{-1}) was used in all of our experiments. Copper specimen grids (200 mesh) with formvar/carbon support film (referred to as TEM grids in the text) were purchased from Beijing XXBR Technology.

2.2 Synthesis of nanoparticles (NPs)

All NPs were prepared by known procedures and stabilized by different ligands in solution. The NPs included citrate-stabilized Au NPs [38] and CTAB-stabilized Au nanorods (Au NRs) [39].

2.3 Encapsulation of Au NPs with $P4VP_{43}$-*b*-PS_{260}-*b*-$P4VP_{43}$

In a typical preparation, 3 mL as-synthesized citrate-stabilized Au NPs were purified and then separated by centrifugation. The isolated NPs were re-dispersed in a DMF solution of ligand **1** (700 μL, 0.11 mg/mL). The solution was then incubated at 60 °C for 2 h, allowing ligand exchange on the surface of AuNPs. Then, in a 4 mL vial, an alliquot (350 μL) of this solution was added to a DMF solution of $P4VP_{43}$-*b*-PS_{260}-*b*-$P4VP_{43}$ (450 μL, 0.71 mg/mL). Finally, 100 μL of H_2O was added to the mixture to give total volume of 900 μL, where the DMF/H_2O volume ratio was 8:1 and concentration of $P4VP_{43}$-*b*-PS_{260}-*b*-$P4VP_{43}$ was 0.356 mg/mL. The mixture was heated at 110 °C for 2 h and then allowed to slowly cool down to room temperature.

For obtaining other DMF/H_2O ratios, the total volume (900 μL) and amounts of Au NPs and $P4VP_{43}$-*b*-PS_{260}-*b*-$P4VP_{43}$ were kept unchanged; only the amount of H_2O and the DMF used in the polymer solution were modified. For encapsulating CTAB-stabilized Au NRs, the as-synthesized NRs were purified to remove the excess CTAB and then isolated by centrifugation. The product was then used in the above procedure in place of the Au NPs.

2.4 Adsorption of small Au NPs on P4VP-PS-P4VP cylinders

The preparation of P4VP-PS-P4VP cylinders (without Au NPs) was adapted from literature [40]. A dioxane solution of the polymer (750 μL, 2.13 mg/mL) was slowly added with 250 μL of deionized water. The cylindrical micelles were obtained after the solution was kept stirring at room temperature for 1 day. Then, a large amount of water (pH 4) was added to the solution (100 μL aliquot of the solution was diluted in 1.4 mL). After centrifugation, the isolated product can be directly used.

The small Au NPs was prepared as follows [41]: 12 μL of 80% THPC and 0.25 mL of 2 M NaOH were added to 45 mL of DI water. The mixture was stirred vigorously for 5 min before 2.0 mL of 1% $HAuCl_4$ was quickly introduced in one shot. An immediate color change to dark brown was observed. This solution was stored in a lightproof container with stirring overnight.

The isolated polymer cylinders were mixed with 1.0 mL solution of the small Au NPs, followed by 6 h incubation. The product was isolated by centrifugation and then characterized.

2.5 "Polymerization" of Au@P4VP-PS-P4VP

The method used here was adapted from our previous report [35]. The purified monomers Au@P4VP-PS-P4VP were dispersed into a DMF/H_2O solution (0.4 mL, V_{DMF}/V_{H2O} = 3:1). NaOH (5 μL, 10 mM) was then added into the solution to reduce the charge repulsion among the coronal blocks, and the final concentration is $[NaOH]_{final}$ = 0.125 mM. The mixture was incubated at 70 ^oC for 2 h to facilitate the "polymerization" of the monomers into chains.

2.6 Characterization

TEM images were collected from a JEM-1400 Transmission Electron Microscope (JEOL) operated at 100 kV. $(NH_4)_6Mo_7O_{24}$ was used as the negative stain in all of the TEM images in this study. TEM grids were treated with oxygen plasma in a Harrick plasma cleaner/sterilizer for 1 min to improve their surfaces hydrophilicity. A drop of sample solution was carefully mixed with the stain solution ($(NH_4)_6Mo_7O_{24}$, 1 *wt*%). Then, the hydrophilic surface of the TEM grid was placed in contact with the stained sample solution, and a filter paper was used to wick off the excess solution from the TEM grid. After drying in air for several h, it can be used for TEM characterization.

UV-Vis spectra were collected on a Cary 100 UV-Vis spectrophotometer.

Raman spectra were collected from the sample solution in a 4 mL glass vial on a PeakSeeker Pro spectrometer (Raman Systems) using a red laser (λ = 785 nm) at 290 mW.

3 Results and Discussion

3.1 Encapsulating Au NPs with $P4VP_{43}$-*b*-PS_{260}-*b*-$P4VP_{43}$

The encapsulation method was based on our previous mechanistic studies and adapted from a published method [31]. Reaction conditions were modified to accommodate the unique properties of the positively charged polymer. In a typical experiment, the purified citrate-stabilized Au NPs [38] were treated with

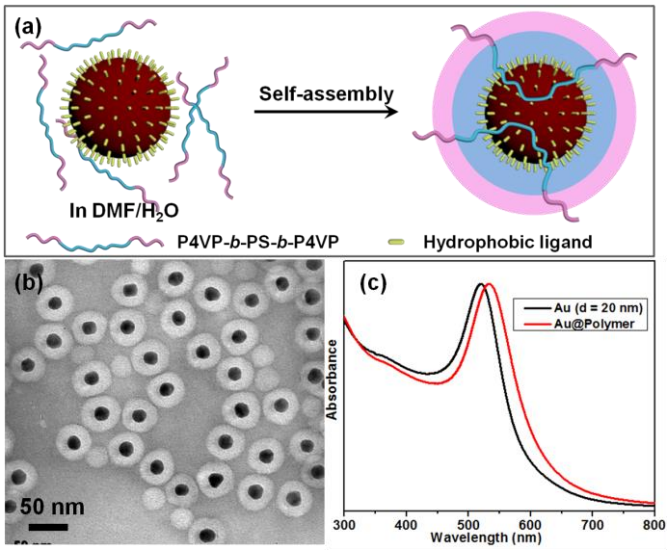

Fig. 1 (a) Schematics showing the preparation and structure of Au@P4VP-PS-P4VP. (b) TEM image of the Au@P4VP-PS-P4VP NPs (d_{Au} = 20 nm). (c) UV-Vis spectra of the sample before and after encapsulating the Au NPs with P4VP-PS-P4VP shells.

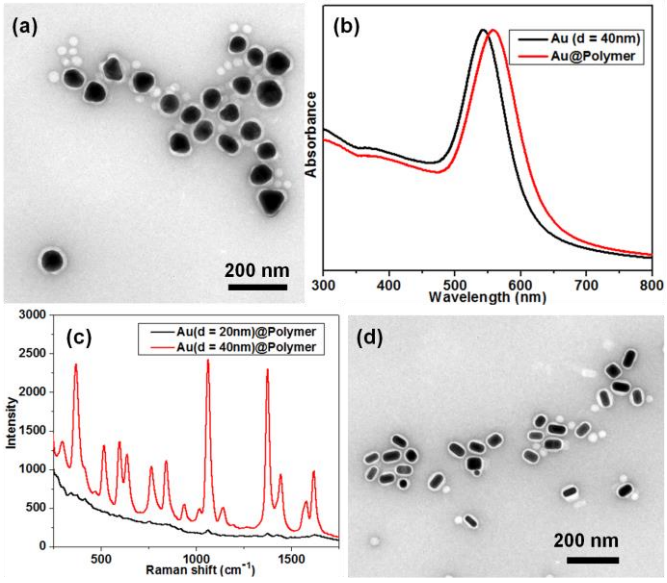

Fig. 2 (a) TEM image of 40 nm AuNPs encapsulated by P4VP-PS-P4VP. (b) UV-Vis spectra of citrate-AuNPs before and after encapsulating with P4VP-PS-P4VP. (c) SERS spectra of 20 nm and 40 nm AuNPs@P4VP-PS-P4VP. (d) TEM image of CTAB-Au nanorods encapsulated by P4VP-PS-P4VP.

hydrophobic ligand **1** at 60 °C for 2 h, to ensure sufficient adsorption of ligand **1**. Then, the functionalized Au NPs were mixed with $P4VP_{43}$-*b*-PS_{260}-*b*-$P4VP_{43}$. The sample was heated in DMF/H_2O solution (v/v = 8:1) at 110 °C for 2 h, to ensure sufficient mobility of the polymer (PS is glassy at high water content solutions) and sufficient time for the polymer self-assembly. After cooling, a large amount of water (pH 4) was added to the sample. As DMF escapes, the polymer domain becomes glassy, locking the polymer structures at kinetically stable states. Thus, after centrifugation, the isolated product can be directly dried at room temperature (there is no need for chemical crosslinking or cryogenic conditions) and characterized by transmission electron microscopy (TEM).

The ligands **1** and **2** were chosen such that the –SH group can anchor on the Au surface and the hydrophobic tail can render the Au surface amenable for the adsorption of the hydrophobic PS blocks. In other words, the strong hydrophobic and van der Waals interactions between the PS and the modified Au surface are of critical importance for reducing the Au-PS interfacial energy, otherwise partial encapsulation will ensue (see SI) [14-15, 31, 42]. The solvent (DMF/H_2O = 8:1) was chosen to cause significant swelling of the polymer and enhance its mobility. The solvent ratio was optimized: higher DMF content would require higher polymer concentration because of its higher solubility (critical micelle concentration); lower DMF content would lead to insufficient mobility of the PS blocks (dependent on their length) and thus unsuccessful encapsulation. The pH = 4 solution was used to ensure sufficient protonation of the pyridine moieties in the P4VP blocks. The resulting surface charge density preserves the structural stability of the polymer shells and prevents the aggregation of NPs.

Figure 1b shows the product core-shell NPs, where each NP consists of one Au core and a uniform polymer shell (d_{Au} = 20 nm). The percentage of singly encapsulated NPs was at around 92.6% (out of the 300 NPs surveyed), with few dimers and trimers (see SI). The Au@P4VP-PS-P4VP NPs were very stable. After repeated centrifugation, there was no obvious change of the sample under TEM. The purified NPs can be easily dispersed in an aqueous solution, indicating the presence of the hydrophilic P4VP blocks on their surface.

From UV-Vis spectra (Figure 1c), the plasmon absorption of the Au@P4VP-PS-P4VP was only slightly red-shifted (533 nm) from that of the citrate-stabilized AuNPs in water (520 nm). As known in the literature [13-14, 43], this shift is a result of the increase of the refractive index of the surrounding medium, which leads to a decrease in the surface plasmon resonance energy. The absence of prominent peaks/shoulders at longer wavelength provides additional support that there were few aggregates of Au NPs in the sample.

In addition to citrate-stabilized Au NPs, CTAB-stabilized Au NRs also can be encapsulated with P4VP-PS-P4VP. As shown in Figure 2d, the core-shell Au-NR@P4VP-PS-P4VP consists of one Au NR and a conformal polymer shell.

3.2 Analysis of core-shell nanostructures

As discussed above, the modification of NPs with hydrophobic ligands is critical for tuning the NP-polymer interfacial energy [31]. To probe the presence of the hydrophobic ligand on the surface of Au NPs, the surface-enhanced Raman scattering (SERS) active ligand **2** was used in place of ligand **1**. In addition, we used large (d_{Au} = 40 nm) Au NPs for stronger SERS signals. As shown in Figure 2a, each Au NP was covered by a uniform polymer layer and there was no obvious aggregation. The UV-Vis spectra further supported this observation (Figure 2b). The Raman signals collected from the solution (not dried samples) were strong and highly reproducible (Figure 2c). They were fully consistent with those reported in the literature [44-45], supporting the presence of SERS-active **2** directly on the Au surface.

On the basis of the hydrophobically functionalized Au surface and its favourable interactions with the hydrophobic PS blocks, we believe that the PS blocks of P4VP-PS-P4VP should adsorb on the Au surface, whereas both of the P4VP blocks should dissolved in the solution facing outwards (Figure 1a). Indirect evidence for the surface P4VP blocks is the high aqueous stability of the core-shell NPs. To further probe the surface pyridine groups, we prepared cylindrical micelles of P4VP-PS-P4VP [40] and incubate them with THPC-stabilized Au NPs (ca. 2 nm). As shown in Figure 3a, the

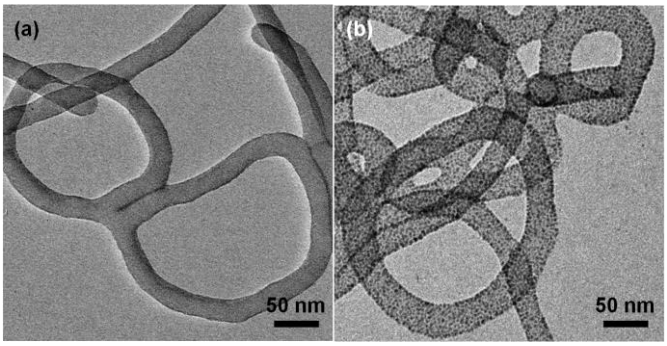

Fig. 3 TEM images showing (a) the cylindrical micelles obtained from the self-assembly of P4VP-PS-P4VP and (b) small AuNPs sticked to the surface of the cylindrical micelles.

surface of the original micelles was smooth and after mixing the cylindrical micelles with the smaller THPC-stabilized AuNPs, the surface of micelles became rough, where a uniform layer of small Au NPs could be identified (Figure 3b). The ligand coordination between the micelles and smaller AuNPs further supported that the positively charged P4VP blocks were covering the outer surface of the polymer shell.

As shown in Figure 1a, the formation of core-shell nanostructure with the PS block facing the Au and both of the P4VP blocks facing the solution is thermodynamically favoured. The driving force is provided by the phase segregation of the hydrophobic and hydrophilic blocks, the affinity between the PS blocks and the ligand-modified Au surface, and the polar interactions between the P4VP blocks with the solvent. Under encapsulation conditions, the polymer undergoes multiple cycles of assembly, disassembly, and shape transformation for sufficient amount of time, so that the system reaches near equilibrium conditions [46]. The exact kinetic pathway of how the polymer molecules find the Au core is thus of less importance. After the core-shell NPs were isolated and diluted in pH 4 solution, the deswollen PS turned glassy, trapping the polymer shell in a kinetically stable state, whereas the protonated P4VP blocks provide surface charge density preventing the aggregation of the core-shell NPs.

3.3 Complex nanostructures of Au@P4VP-PS-P4VP

In the absence of Au NPs, the self-assembly of BCPs is known to give different micelle morphologies depending on the solvent ratio. Basically, there is a competition between the surface energy (small surface to volume (S/V) ratio means low surface energy) and the repulsion among the surface P4VP blocks. Small spherical micelles have large curvature (weak repulsion) but large S/V ratio, whereas large vesicles have small curvature and small S/V ratio. Thus, lower DMF content of the solvent drives the micelles towards vesicles because a lower degree of swelling increases the polymer-solvent interfacial energy (the deswollen domain is more dissimilar to the solvent) [46-47].

In the presence of hydrophobically functionalized Au NPs, the self-assembly of P4VP-PS-P4VP gave rise to various type of micelles with embedded Au NPs. The purified samples after removing the empty micelles (those without Au NPs) were shown in the following. When the DMF/H_2O ratio was 8:1, core-shell spherical micelles were obtained (Figure 4a). When the water content was increased to DMF/H_2O = 6:1, a few cylindrical micelles with embedded Au NPs emerged (Figure 4b). The amount of cylinders increased when the DMF/H_2O reached 4:1 (Figure 4c). Further increase the water amount (DMF/H_2O = 3:1) gave vesicles

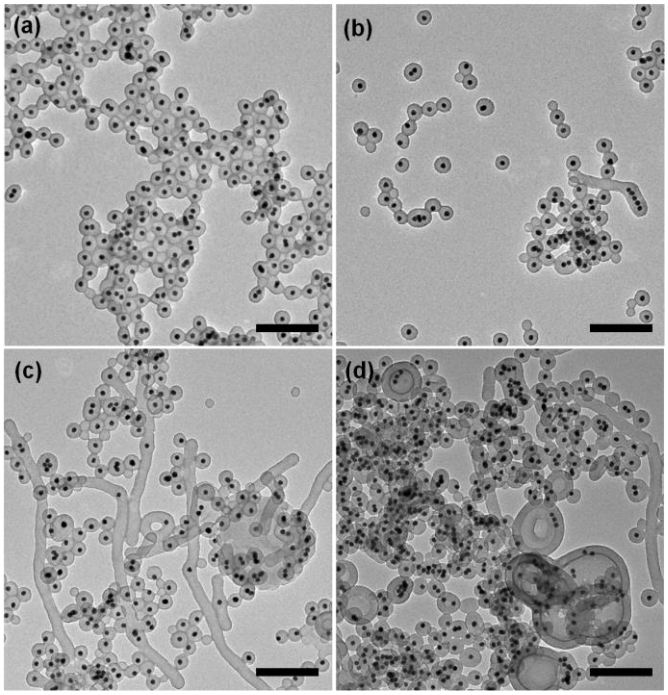

Fig. 4 TEM images of different morphologies of AuNPs@ P4VP-PS-P4VP obtained in different ratios of DMF/H_2O: (a) 8:1, (b) 6:1, (c) 4:1 and (d) 3:1. Scale bar: 200 nm.

with embedded Au NPs (Figure 4d). It is important to note that in Figure 4c-d, many Au@P4VP-PS-P4VP remained as simple spheres, whereas only a few nanostructures were able to undergo multiple aggregation and coalescence processes to form the large cylinders and vesicles.

3.4 "Polymerization" of Au@P4VP-PS-P4VP

In our previous work, we showed a unique property of the Au@PSPAA core-shell NPs, namely that they could undergo "chain-growth polymerization" to form long chains. It is of importance to know if such behaviour is general to other types of BCPs. The Au@P4VP-PS-P4VP provides a nice comparison, because it involves the positively charged triblock copolymer, as opposed to the negatively charged diblock copolymer.

The as-prepared Au@P4VP-PS-P4VP were purified and then dispersed in a DMF/water mixture (v/v = 3:1). Then, a small amount of base (0.125 mM NaOH) was added to induce the self-assembly and the mixture was incubated at 70 ^oC for 2 h. Finally, the sample was diluted by a large amount of H_2O (pH 4) and purified by centrifugation. Here, NaOH was used to deprotonate the positively charged P4VP blocks and reduce their repulsion, with a similar effect as the addition of HCl to PSPAA micelles. The low DMF content solution was also used to drive the micelles towards cylinders. In this set of experiments, the Au@P4VP-PS-P4VP NPs were pre-fabricated and the empty micelles have been removed. Thus, the Au/polymer ratio was much higher than those in the Figure 4.

In the product, some Au@P4VP-PS-P4VP NPs polymerized to form chains while many others remained as the monomers (Figure 5). Most of the chains were unbranched with a polymer shell covering their surface, and they have a typical length of 3–20 NPs. The very long chains were rarely observed (Figure 5b). The fact that a few chains were able to aggregate multiple times whereas most other cannot is characteristic of chain growth polymerization mode. In contrast, in the step-growth mode, the monomers are quickly

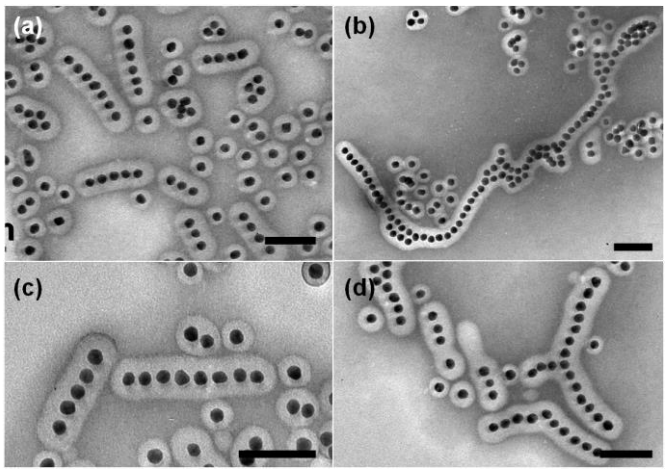

Fig. 5 TEM images showing the NP chains made from the "polymerization" of AuNPs@P4VP-PS-P4VP "monomers". Scale bar: 100 nm.

consumed giving dimers, trimers, and larger clusters. Thus, the high percentage of the remaining monomers is inconsistent with the step-growth mode. The length of the "polymer" chains is governed by the intrinsic slow rate of NP aggregation, which is very different from the rapid reaction rates of radicals in organic polymerization.

While we cannot easily characterize the underlying process, the chain growth polymerization behaviour appears to be general for very different copolymer systems, namely Au@P4VP-PS-P4VP and Au@PSPAA. We speculate that disorganized (not fully phase segregated) polymer domain may enhance the probability of successfully aggregation, leading to more disorganized domains at the growing end of the chain and thus promoting further reactions.

4 Conclusions

In summary, we showed that the encapsulation method, the co-assembly to form hybrid cylinders and vesicles, and the "chain-growth polymerization" can work using a positively charged amphiphilic triblock copolymers (P4VP-PS-P4VP). These results were important support for the general principles that we have established previously for Au@PSPAA system. With great stability and well controlled hybrid nanostructures, the positively charged Au@P4VP-PS-P4VP NPs are expected to be a nice addition to the negatively charged Au@PSPAA, in the future construction of more complex nanostructures.

References

1. L. F. Zhang, A. Eisenberg, Science **268**, 1728 (1995)
2. D. E. Discher, A. Eisenberg, Science **297**, 967 (2002)
3. T. Smart, H. Lomas, M. Massignani, M. V. Flores-Merino, L. R. Perez, G. Battaglia, Nano Today **3**, 38 (2008)
4. L. F. Zhang, K. Yu, A. Eisenberg, Science **272**, 1777 (1996)
5. L. F. Zhang, A. Eisenberg, J. Am. Chem. Soc. **118**, 3168 (1996)
6. M. Antonietti, S. Förster, Adv. Mater. **15**, 1323 (2003)
7. Y. Y. Mai, A. Eisenberg, Chem. Soc. Rev. **41**, 5969 (2012)
8. N. L. Rosi, C. A. Mirkin, Chem. Rev. **105**, 1547 (2005)
9. P. Alivisatos, Nat. Biotech. **22**, 47 (2004)
10. M. Han, X. Gao, J. Z. Su, S. Nie, Nat. Biotech. **19**, 631 (2001)
11. X. Michalet, F. F. Pinaud, L. A. Bentolila, J. M. Tsay, S. Doose, J. J. Li, G. Sundaresan, A. M. Wu, S. S. Gambhir, S. Weiss, Science **307**, 538 (2005)
12. I. L. Medintz, H. T. Uyeda, E. R. Goldman, H. Mattoussi, Nat. Mater. **4**, 435 (2005)
13. Y. Kang, T. A. Taton, Angew. Chem. Int. Ed. **44**, 409 (2005)
14. H. Y. Chen, S. Abraham, J. Mendenhall, S. C. Delamarre, K. Smith, I. Kim, C. A. Batt, ChemPhysChem **9**, 388 (2008)
15. T. Chen, M. X. Yang, X. J. Wang, L. H. Tan, H. Y. Chen, J. Am. Chem. Soc. **130**, 11858 (2008)
16. B. Dubertret, P. Skourides, D. J. Norris, V. Noireaux, A. H. Brivanlou, A. Libchaber, Science **298**, 1759 (2002)
17. N. Liu, B. S. Prall, V. I. Klimov, J. Am. Chem. Soc. **128**, 15362 (2006)
18. T. Chen, G. Chen, S. Xing, T. Wu, H. Chen, Chem. Mater. **22**, 3826 (2010)
19. H. Sun, J. He, J. Wang, S.-Y. Zhang, C. Liu, T. Sritharan, S. Mhaisalkar, M.-Y. Han, D. Wang, H. Chen, J. Am. Chem. Soc. **135**, 9099 (2013)
20. S. Förster, M. Antonietti, Adv. Mater. **10**, 195 (1998)
21. A. Fahmi, T. Pietsch, C. Mendoza, N. Cheval, Mater. Today **12**, 44 (2009)
22. M. Moffitt, H. Vali, A. Eisenberg, Chem. Mater. **10**, 1021 (1998)
23. B. S. Kim, J. M. Qiu, J. P. Wang, T. A. Taton, Nano Lett. **5**, 1987 (2005)
24. Y. J. Kang, T. A. Taton, Angew. Chem. Int. Ed. **44**, 409 (2005)
25. Y. J. Kang, T. A. Taton, Macromolecules **38**, 6115 (2005)
26. A. R. Herdt, B.-S. Kim, T. A. Taton, Bioconjugate Chem. **18**, 183 (2006)
27. Y. Kang, T. A. Taton, J. Am. Chem. Soc. **125**, 5650 (2003)
28. Y. Mai, A. Eisenberg, J. Am. Chem. Soc. **132**, 10078 (2010)
29. Y. Y. Mai, A. Eisenberg, Macromolecules **44**, 3179 (2011)
30. Y. Liu, Y. Li, J. He, K. J. Duelge, Z. Lu, Z. Nie, J. Am. Chem. Soc. **136**, 2602 (2014)
31. H. Wang, L. Chen, Y. Feng, H. Chen, Acc. Chem. Res. **46**, 1636 (2013)
32. L. H. Tan, S. X. Xing, T. Chen, G. Chen, X. Huang, H. Zhang, H. Y. Chen, ACS Nano **3**, 3469 (2009)
33. G. Chen, Y. Wang, L. H. Tan, M. X. Yang, L. S. Tan, Y. Chen, H. Y. Chen, J. Am. Chem. Soc. **131**, 4218 (2009)
34. H. Wang, J. Xu, J. Wang, T. Chen, Y. Wang, Y. W. Tan, H. Su, K. L. Chan, H. Chen, Angew. Chem.-Int. Edit. **49**, 8426 (2010)
35. H. Wang, L. Y. Chen, X. S. Shen, L. F. Zhu, J. T. He, H. Y. Chen, Angew. Chem.-Int. Edit. **51**, 8021 (2012)
36. C. Liu, G. Chen, H. Sun, J. Xu, Y. Feng, Z. Zhang, T. Wu, H. Chen, Small **7**, 2721 (2011)
37. C. Liu, L. Yao, H. Wang, Z. R. Phua, X. Song, H. Chen, Small, 1332 (2013)
38. G. Frens, Nature-Physical Science **241**, 20 (1973)
39. N. R. Jana, L. Gearheart, C. J. Murphy, J. Phys. Chem. B **105**, 4065 (2001)
40. H. Z. Yu, W. Jiang, Macromolecules **42**, 3399 (2009)
41. H. Zhang, Y. J. Li, I. A. Ivanov, Y. Q. Qu, Y. Huang, X. F. Duan, Angew. Chem.-Int. Edit. **49**, 2865 (2010)
42. S. Torza, S. G. Mason, J. Colloid Interface Sci. **33**, 67 (1970)
43. Y. Zheng, M. Xiao, S. Jiang, F. Ding, J. Wang, Nanoscale **5**, 788 (2013)
44. J. K. Yoon, K. Kim, K. S. Shin, J. Phys. Chem. C **113**, 1769 (2009)
45. R. A. Alvarez-Puebla, D. S. Dos Santos, R. F. Aroca, Analyst **129**, 1251 (2004)
46. Y. Wang, J. He, C. Liu, W. H. Chong, H. Y. Chen, Angew. Chem.-Int. Edit. **Accepted** (2014)
47. L. Chen, H. Shen, A. Eisenberg, J. Phys. Chem. B **103**, 9488 (1999)

Comment by Reviewer # 1

The article "Encapsulation of Au Nanoparticles by P4VP-PS-P4VP for Controlled Chain Assembly" describes the complex nanostructures formed by the self-assembly of Au nanoparticles covered by amphiphilic block-copolymers with the PS block as a core and the positive charged P4VP block as a shell. The present work is indeed a nice extension of the recent works of Chen's group. The article is well written and easy to follow. The experiments are well executed and the drawn conclusions are valid except the part in the "Polymerization" section. There are no further technical issues to address and only some minor issues and comments arise:

Question 1. To further support the author's conclusion that "the PS blocks of P4VP-PS-P4VP should adsorb on the Au surface, whereas both of the P4VP blocks should dissolved in the solution facing outwards", the authors can run a control experiment with just P4VP homo-polymers, and compare to the result of using the block copolymers.

Response:

P4VP is soluble in water and its pyridine groups can bind to the Au surface. Such a polymer is highly swollen by the solvent and can only loosely bind to the Au surface, in contrast to the compact polymer domain formed by the phase-segregated, hydrophobic PS blocks. Indeed, in the images reported in our manuscript, only the PS domain appeared as the while polymer shells, whereas the P4VP layer has the similar contrast with the background and hard to distinguish. As shown in previous works, the PAA blocks do not contribute the polymer shell thickness as displayed in the TEM images of PSPAA micelles.

An additional problem with homo-P4VP is that each polymer chain could bind to multiple Au NPs, and each Au NP can be linked to multiple polymer chains. As such, the P4VP can cause the aggregation of Au NPs. This is in contrast to our system, where the –SH ended ligand, being stronger, can shield the Au surface. The phase segregation of amphiphilic block copolymer P4VP-PS-P4VP gave rise to orderly PS and P4VP domains, encapsulating the NPs and preventing their aggregation.

Question 2. In the "polymerization of Au@P4VP-PS-P4VP" section, the authors observed that "Most of the chains were unbranched with a polymer shell covering their surface, and they have a typical length of 3-20 NPs. The very long chains were rarely observed (Figure 5b)." This observation is indeed more like the behavior of step-growth polymerization, instead of chain polymerization. In chain polymerization, the chain grows very fast, and only very long chains and monomers can be observed, that is, it is hard to find short chains. In the contrast, for step-growth polymerization, the chain distribution follows the Flory distribution. At low conversion when a large portion of monomer is still present, the population of monomers and short chains are always more than longer chains, and it is very hard to find very long chains, which most likely form at high conversion.

Response: We thank the reviewer for the insightful comments. The short “polymer” chains in our system were due to the intrinsic slow rate of NP aggregation, not a mistake in assigning the growth mode.

The following table gives a clear comparison between the step and chain growth mechanisms. In step growth mechanism, all monomers react with each other and with oligomers with the same rate. Thus, monomers quickly turned into dimers, trimers and then short oligomers. At low conversion when a large portion (>30%) of monomer is still present, the products are mostly dimers and trimers (*Nano*

Letters, **2008**, 8, 2643-2647). By the time short chains (7~10 NPs) are formed, the monomers have been nearly depleted. In chain growth mechanism, the active species (radical or reactive group) can react multiple times while the monomers cannot react with each other. Thus, long chains can form while most of the monomers remain.

In our system, the aggregation is not extensive, giving rise to short oligomers (5-10). But the large percentage of monomers and **the small percentage of dimers and trimers** indicate that the mechanism is chain-growth mode.

Step vs. Chain-Growth

Step-Growth	Chain-Growth
1. Proceed by stepwise intermolecular mechanism, which is the same for all reactions.	1. Proceed by a kinetic chain reaction mechanism. (C-G refers to the mechanism, not the polymer.)
2. Monomers react with each other or any size oligomer or polymer.	2. C-G reactions are initiated by an external source (catalyst, energy, etc.).
3. All functional groups of equal reactivity,whether on monomer, oligomer, or polymer.	3. Monomers react only with active center (radical, ion) of growing chain, not each other.
4. High % conversion is necessary to produce high MW polymers.	4. Polymers grow at a rapid rate and can readily attain high MW values.
5. Most are equilibrium-controlled and all FG species affect distribution.	5. Mechanism involves initiation, propagation & termination, which proceed at different rates.

Question 3. Caption of Fig. 1, it should be UV-Vis, instead of UV-vis. Caption of Fig. 2, it should be UV-Vis spectra, instead of UV-vis spectrum. Page 4, lift column, line 3, it should be Figure 3b, instead of Figure 3a.

Response:

We have revised these mistakes in the new version.

Comment by Reviewer # 3

Authors reported a new mthod to encapsulate gold NPs in an amphiphilic positively charged triblock copolymer (P4VP-PS-P4VP) which is an important complementary to the principle authors's group has established previously. And the text was organized very logically and all the data are solid and persuasive. So i think this is a nice work and deserve to be published asap as it is.

Response:

We thank the reviewer for the high recognition.